NORSAR

NORSAR Scientific Report No. 2-2003

Semiannual Technical Summary

1 January - 30 June 2003

Frode Ringdal (ed.)

Kjeller, August 2003

6.6 Body-Wave Magnitude Residuals of IMS Stations

6.6.1 Introduction

The body-wave magnitude mb is important in many schemes for discriminating between natural earthquakes and man-made explosions. Observed magnitudes show a large scatter and stations often have a systematic magnitude bias, which makes it difficult to calculate magnitudes in the case of events with only a small number of observations. However, this is the scenario for seismic stations analyzed at the IDC of the CTBTO in Vienna.

The amplitude (and thereby magnitude) observations at the IMS stations must therefore be calibrated. The amplitude measurements in the bulletins of IDC (REBs) have the advantage that they follow common rules and that therefore the scatter due to the application of different digital filters, unknown transfer functions, and analysis rules is reduced compared with the amplitude data in other international catalogues. Today, for many of the IMS stations, thousands of amplitude readings are now available for a systematic analysis of the station bias.

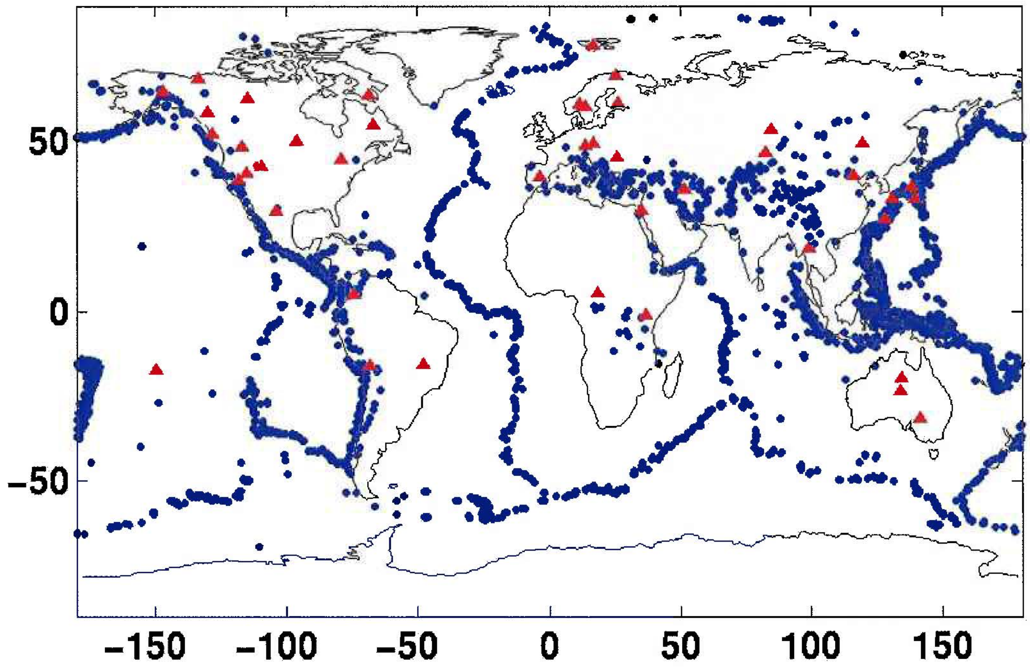

Fig. 6.6.1. Map of all crustal events between 1 January 1995 and 28 February 2003 with a reported Harvard M_0 value (blue points) and of all IMS stations investigated in this study (red triangles).

6.6.2 Data Base

The basic data set used, is the set of the amplitude and period measurements of first P onsets as published since 1995 in the REBs by the prototype IDC for the GSETT-3 experiment at CMR in Arlington and later by the IDC of the CTBTO in Vienna. The IMS network of seismic stations was constantly under change. In this study, amplitude observations were only analyzed for stations which are part of the IMS as of June 2003; these stations are plotted on the map in Fig. 6.6.1 as red triangles.

As an independent measure for the size of the analyzed events the seismic moment M_0 is used as published in the Harvard CMT catalogues. For this, all the CMT solutions of events between 1 January 1995 and 28 February 2003 were retrieved from the Harvard CMT web-page (http://www.seismology.harvard.edu/CMTsearch.html). To remove all depth dependent factors in this study only crustal events with a CMT depth <= 33 km were analyzed; all events used in this study are plotted on the map in Fig. 6.6.1 as blue points. Using the known relation between the seismic moment M_0 in [Nm] and the moment magnitude Mw (Kanamori, 1977),

$$Mw = 2/3\ (\log M_0 - 9.1), (1)$$

the magnitudes Mw were calculated for all selected events and compared with the observed body-wave magnitudes m_b. Fig. 6.6.2 shows a histogram of the calculated Mw values of all events used in this study; note that Harvard uses a lower magnitude threshold of about Ms = 5.0 for calculating a CMT solution.

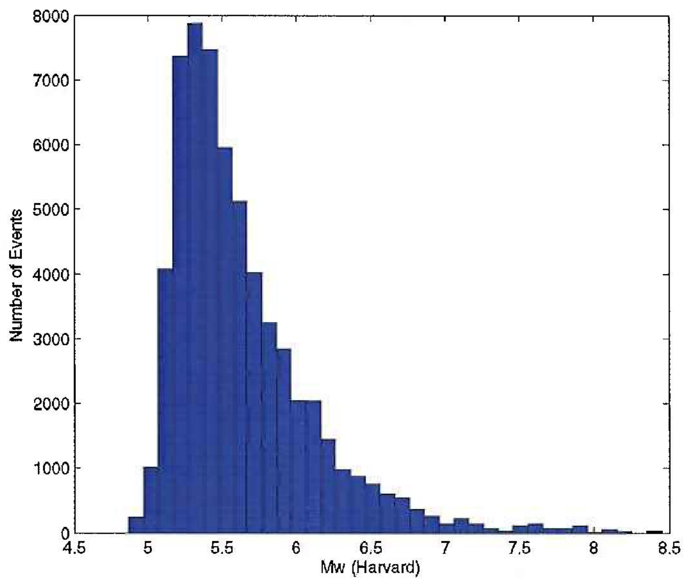

Fig. 6.6.2. Histogram for Mw of the analyzed events calculated from Harvard M_0.

The amplitude-period pairs of the first P onsets reported in the REBs, were used to calculate body-wave station magnitudes m_b for all events with a known M_0. For this, the epicentral distances between the CMT sources and the stations were recalculated and the attenuation relation of Veith and Clawson (1972) was applied.

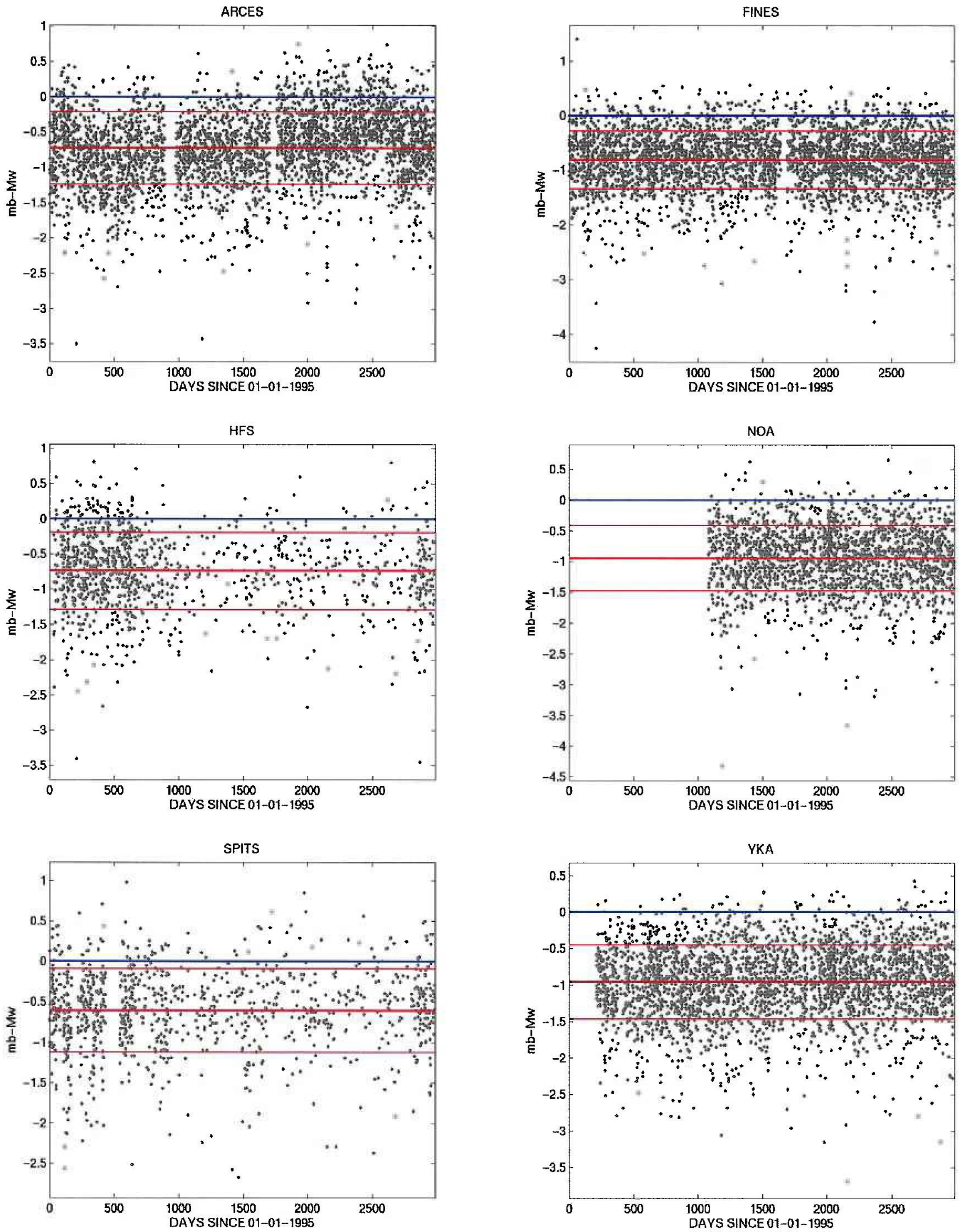

Fig. 6.6.3. Time dependent behavior of station mb observations minus event Mw for some of the stations investigated. The thick red line represents the mean mb bias and the two thin red lines are the +/- one standard deviation limits. The time axis shows days since start of the GSETT-3 experiment on 1 January 1995.

6.6.3 Stability of Magnitude Measurements Over Time

Although the amplitude measuring procedure at the prototype IDC and the IDC was stable over time, the whole IMS network was and is still under construction. Stations were added one by one and, for some, the equipment was changed due to major refurbishment work. Station-response information was always included when it became available at the prototype IDC or IDC, which was not necessarily the same time at which the station's onset readings were included in the REBs. Therefore, the time-dependent behavior of the difference between station m_b observations and the Mw values calculated here, was chosen as an indicator for the stability of the amplitude measurements.

Fig. 6.6.3 shows the result of this analysis for some of the IMS stations. The time scale was chosen to be the number of days since start of the GSETT-3 experiment on 1 January 1995. The thick red line represents the mean m_b bias with respect to Mw and the two thin red lines are the limits of +/- one standard deviation. The calculated bias in the order of about -1 magnitude units is the cumulative effect of the principal offset between the m_b and the Mw scales, and the observed bias between the amplitudes as reported in the REBs and other amplitude reporting stations or institutions (*e.g.*, Granville *et al.*, 2002). However, the m_b-Mw bias is very stable at most stations but shows some jumps at some stations often connected with known refurbishment periods. Assuming that the newest amplitude measurements are free of errors, only data showing the same offset as the newest data were used for further analysis. For ARCES, for example, data were used only from the last 350 days, for FINES, HFS, NOA, and SPITS all shown data were used, and for YKA data from the first 212 days were not used. The data from all other stations were checked and corrected in the same manner.

6.6.4 Distance-Dependent Behavior of Amplitude Measurements

Calculating an event's magnitude involves measuring the amplitude of a seismic phase and correcting this measurement for the attenuation of seismic waves on the path from source to receiver. Different, phase-dependent attenuation relations exist and are used to estimate magnitudes. The relation of Gutenberg and Richter (1956a, b) is most often used for first P onsets. However, this relation does not provide corrections for core phases, which are the first short period P-type onsets beyond about 105 deg epicentral distance. This is not the case for the more modern attenuation relations of Veith and Clawson (1972), who also published amplitude corrections for the PKP range. Therefore, the Veith-Clawson corrections are used to calculate m_b in the REBs and also in this study. With the collection of thousands of amplitude data presented here, it can now be proved that the estimated magnitudes depend on the epicentral distance.

The body wave magnitude m_b is defined as:

$$m_b = \log_{10} (A / T) + \text{corr (delta, depth)},(2)$$

with the measured amplitude A, period T, and distance and depth dependent attenuation correction corr (here from Veith-Clawson). Plotting the difference between Mw and $\log_{10}(A/T)$ for each station will then provide station dependent attenuation values.

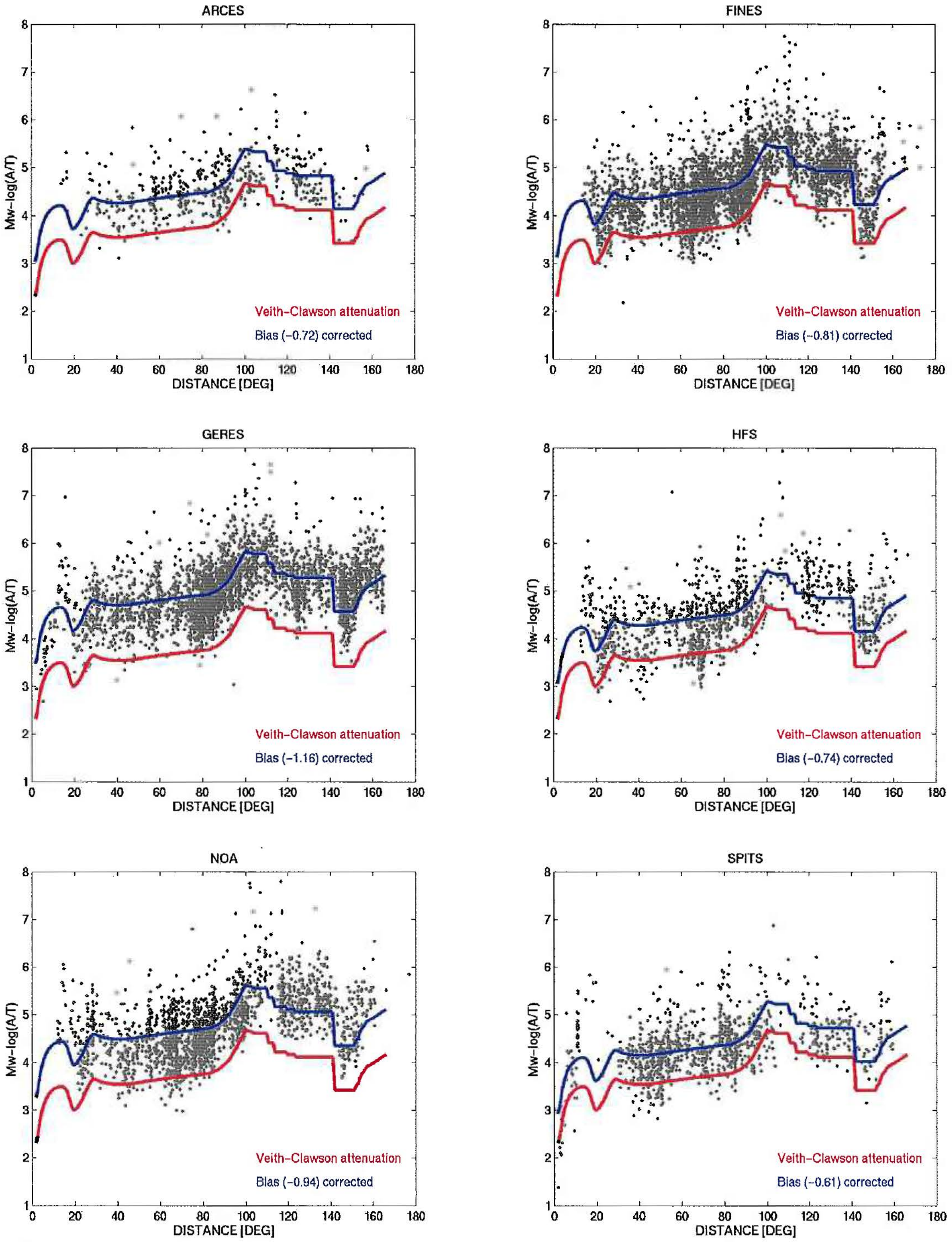

Fig. 6.6.4. Mw - log(A/T) observations for a subset of investigated stations. The red curve is the Veith-Clawson attenuation curve for a surface event (Veith and Clawson, 1972). The blue curves show for each station the Veith-Clawson attenuation after adding the mean station bias.

Fig. 6.6.4 shows a panel with six such observed data sets of (Mw - log(A/T)) for the seismic stations ARCES, FINES, GERES, HFS, NOA, and SPITS. The red curves are always the

Veith-Clawson attenuation curve for a surface event (Veith and Clawson, 1972). Obviously, the observed data do not follow this curve. However, after calculating a mean bias between observations and the Veith-Clawson curve and correcting the attenuation by this constant value of about one magnitude unit, the correspondence becomes quite good for all stations (see the blue lines). The scatter of the data is still large and at some distances very large (*e.g.*, FINES at ca. 90 deg or GERES at about 120 deg) but the general correspondence between the blue lines and the observed data is quite good.

6.6.5 The m_b - Mw Relation

A known phenomenon is that the m_b scale saturates for magnitudes above about 6.5. Therefore, m_b residuals for events with larger magnitudes are not only the effect of station and ray-path anomalies but also of this saturation effect. To define an upper magnitude limit, all station m_b values defined in equation (2) were corrected with the constant bias (stcorr) as calculated for Fig. 6.6.4:

$$m_b = \log_{10} (A / T) + \text{corr (delta, depth)} + \text{stcorr} \quad (3)$$

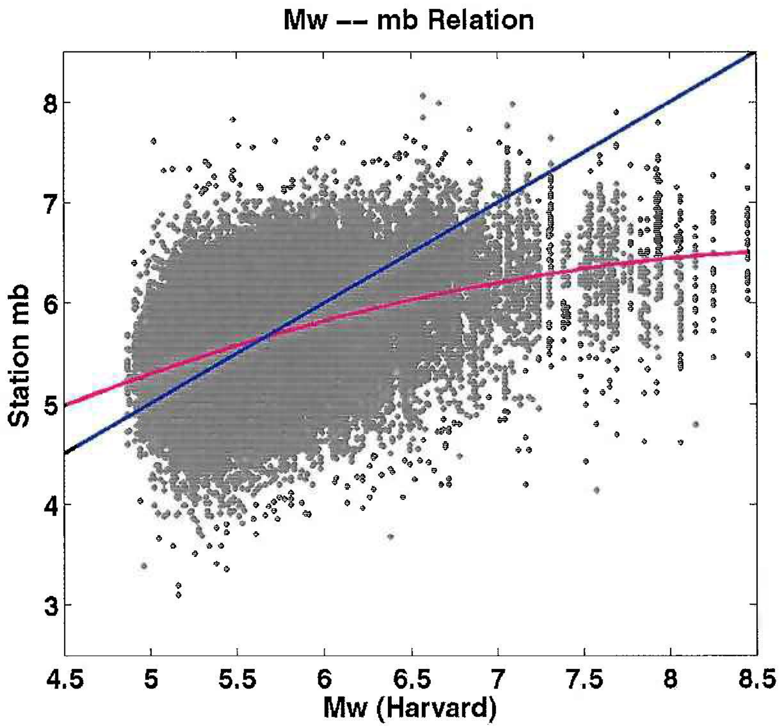

Fig. 6.6.5. All station bias corrected mb values plotted with respect to Mw as calculated from the Harvard CMT solutions. The blue line represents identity between mb and Mw, the mangenta line follows the calculated 2nd order polynomial describing the relation between m_b and Mw.

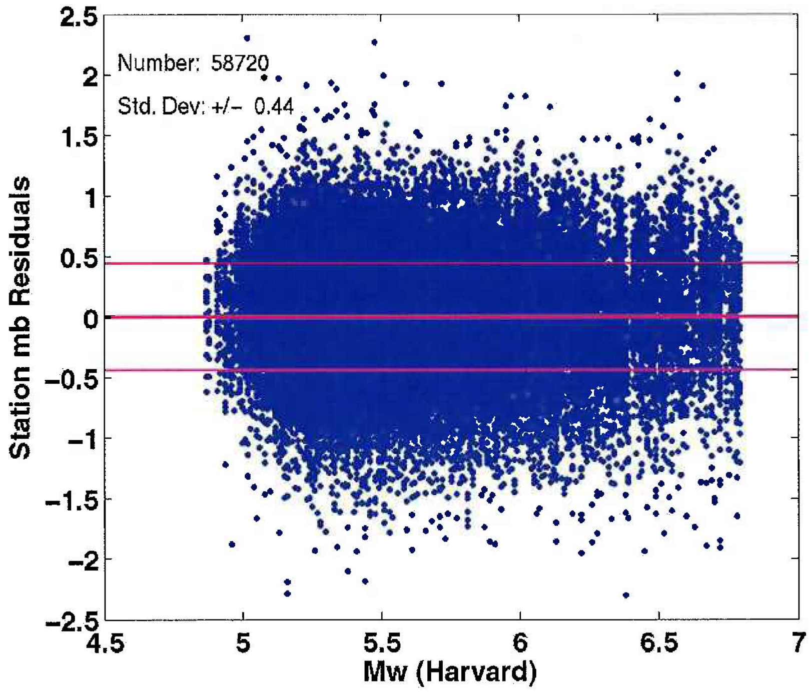

Fig. 6.6.6. Station mb residuals after removing the fitted 2nd order polynomial. The two thin mangenta lines give the +/- one standard deviation range.

These 60 273 new m_b values are plotted in Fig. 6.6.5 with respect to the corresponding Mw values. The saturation effect is clearly visible, as is the fact that m_b is not identical to Mw for magnitudes below 6.5. In the latter case, the data should be scattered around the blue line. Therefore, the m_b - Mw relation was fitted by a second order polynomial:

$$m_b = -0.0716*Mw^2 + 1.3138*Mw + 0.5171 \quad (4)$$

Because of the saturation effect, which cannot be modelled, only m_b observations for which the event magnitude Mw was <= 6.8, were used for the final analysis. Fig. 6.6.6 shows the remaining residuals for these 58 720 m_b observations. The standard deviation of +/- 0.44 magnitude units for all m_b observations can be attributed to a number of different effects: focusing and defocusing structures along the ray paths between source and receiver, wrong hypocenter determinations (in particular uncertainty of focal depth), the influence of the radiation pattern on P-wave amplitudes as shown in Schweitzer and Kværna (1999), distance depending modelling errors of the applied Veith-Clawson attenuation curve (*e.g.*, recently Rezapour (2003) published new attenuation values for teleseismic P onsets), some still not detected instrumentation errors, and other data-analysis errors such as incorrect phase associations.

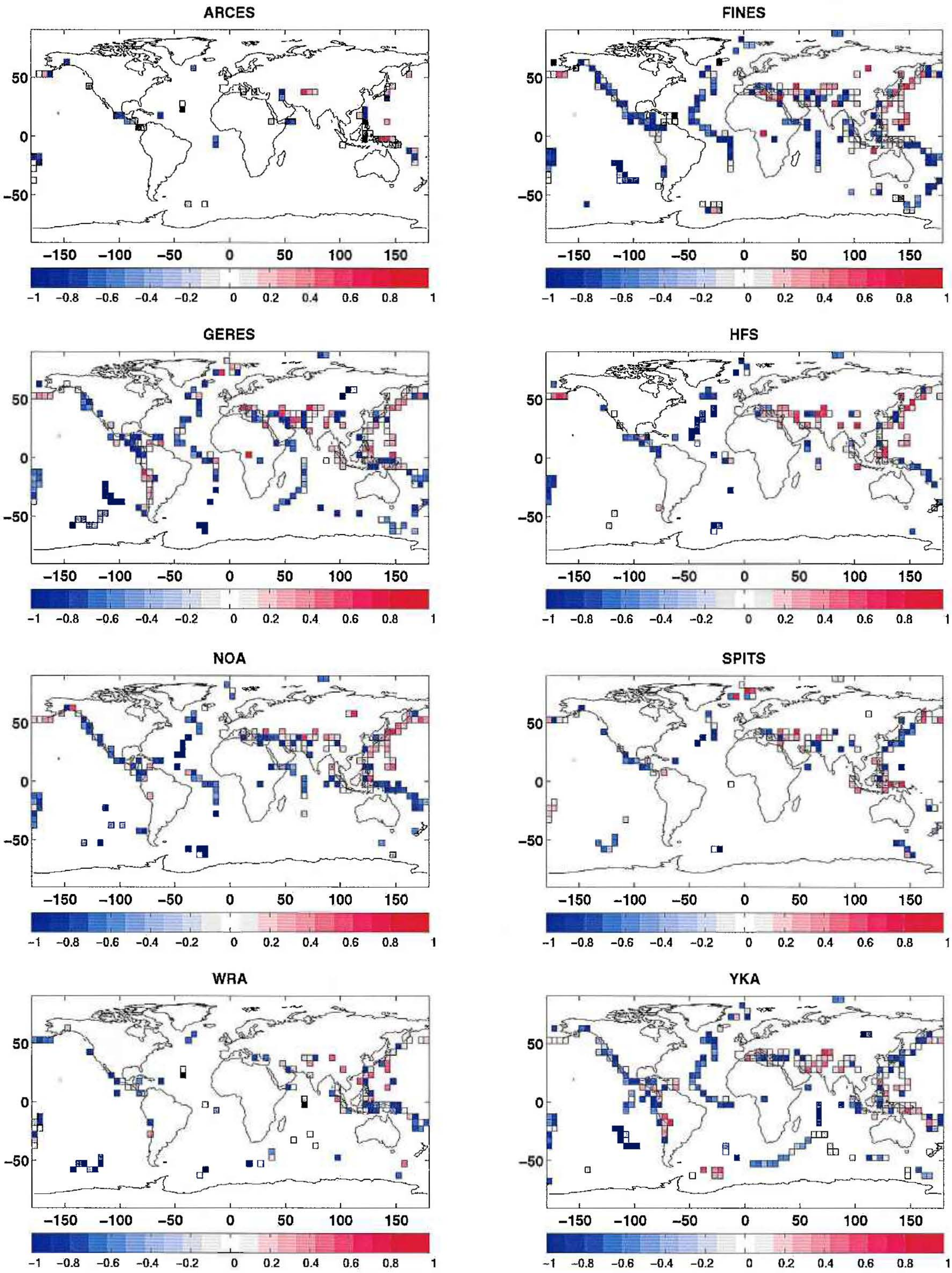

Fig. 6.6.7. Geographical distribution of mean m_b residuals for a subset of the investigated stations.

6.6.6 Geographical Distribution of the Residuals

If systematic effects like ray path and double couple radiation have a major contribution the residuals as derived in Section 6.6.5 and plotted in Fig. 6.6.6, the residuals should show some systematic geographical distribution. Therefore, the observed residuals were binned in 5 deg x 5 deg bins with respect to their epicenter for each station separately and mean values were plotted on maps. Fig. 6.6.7 shows such maps for eight of the investigated stations. The mean m_b residuals are only plotted for bins with at least three observations. The distribution of bins reflects the sensitivity of the different stations with respect to specific source regions and the usage of auxiliary stations like SPITS and HFS. However, for all stations, the regions with positive (red) and negative (blue) magnitude residuals show systematic patterns. This pattern is not identical for the different stations; *e.g.*, the subduction zones north of Australia have dominantly blue colors at WRA but red colors at SPITS and YKA, the South Sandwich events have negative residuals at GERES and NOA but positive residuals at YKA.

In general the mid-oceanic ridges have a tendency to display negative m_b residuals with respect to the reference magnitude Mw but contrary, mb seems to overestimate the event's size in subduction zones. This is in agreement with the dominant double couple radiation of the different tectonic regions, in particular for the mid-oceanic ridges systems with strike-slip movements and thereby low P-wave radiation down into the mantle.

6.6.7 Conclusions

The REBs contain the most self-consistent database of amplitude and period observations of body waves. These data can be corrected for the mean station bias between m_b and Mw. The remaining m_b - Mw relation can simply be modeled with a 2nd order function. By applying this relation one can derive an expected m_b value for each event and calculate observed station m_b residuals. These residuals are up to about +/- 2 (and standard deviation of about +/- 0.44) magnitude units.

Binning these residuals with respect to their source regions and plotting them on geographical maps clearly show a source region specific pattern. The reasons for this observation will mostly be ray-path dependent attenuation anomalies (defocusing, focusing) and source region dependent dominant double-couple radiation.

The application of source-station specific corrections (SSSCs) for amplitude / period observations is recommended and will result in more stable magnitude estimates. However, this will require more studies on the influence of a mixture of calibrated and uncalibrated areas / stations on network magnitudes.

Johannes Schweitzer

References

Granville, J. P., Kim, W.-Y., and P. G. Richards (2002): An assessment of seismic body-wave magnitudes published by the prototype International Data Centre. Seism. Res. Lett. **73**, 893-906.

Gutenberg, B. and C. F. Richter (1956a): Magnitude and energy of earthquakes. Ann. Geof. **9**, 1- 15.

Gutenberg, B. and C. F. Richter (1956b): Earthquake magnitude, intensity, energy, and acceleration. Bull. Seism. Soc. Amer. **46**, 105-143.

Harvard CMT catalogue for 1995 - 2003: see http://www.seismology.harvard.edu/CMTsearch.html

Kanamori, H. (1977): The energy release in great earthquakes. J. Geophys. Res. **82**, 2981-2987.

Veith, K. F. and G. E. Clawson (1972): Magnitude for short period P-wave data. Bull. Seism. Soc. Amer. **72**, 435-452.

Rezapour, M. (2003): Empirical global depth-distance correction terms for m_b determination based on seismic moment. Bull. Seism. Soc. Amer. **93**, 172-189.

Schweitzer, J and T. Kværna (1999): Influence of source radiation patterns on globally observed short-period magnitude estimates (m_b). Bull. Seism. Soc. Am. **89**, 342-347.